Cardiac Mitochondrial PTEN-L determines cell fate between apoptosis and survival during chronic alcohol consumption

Anusha Sivakumar[1] · Suresh Shanmugarajan[1] · Ramasamy Subbiah[1] · Rekha Balakrishnan[1]

Abstract

Chronic alcohol consumption induces myocardial damage and a type of non-ischemic cardiomyopathy termed alcoholic cardiomyopathy, where mitochondrial ultrastructural damages and suppressed fusion activity promote cardiomyocyte apoptosis. The aim of the present study is to determine the role of mitochondrial fission proteins and/or other proteins that localise on cardiac mitochondria for apoptosis upon ethanol consumption. In vivo and in vitro chronic alcohol exposure increased mitochondrial Drp1 levels but knockdown of the same did not confer cardioprotection in H9c2 cells. These cells displayed downregulated expression of MFN2 and OPA1 for Bak-mediated cytochrome c release and apoptosis. Dysregulated PTEN/AKT cell survival signal in both ethanol treated and *Drp1* knockdown cells augmented oxidative stress by promoting mitochondrial PTEN-L and MFN1 interaction. Inhibiting this interaction with VO–OHpic, a reversible PTEN inhibitor, prevented Bak insertion into the mitochondria and release of cytochrome c to cytoplasm. Thus, our study provides evidence that Drp1-mediated mitochondrial fission is dispensable for ethanol-induced cardiotoxicity and that stress signals induce mitochondrial PTEN-L accumulation for structural and functional dyshomeostasis. Our in vivo results also demonstrates the therapeutic potential of VO–OHpic for habitual alcoholics developing myocardial dysfunction.

Keywords Mitochondrial fission · Alcohol · Heart · MOMP · Drp1 silencing · PTEN-L · VO–OHpic

Introduction

Cardiovascular disorders (CVDs) are a major cause of global mortality, and chronic, excessive alcohol consumption is a risk factor for developing or aggravating myocardial dysfunction. It is a complex relationship between alcohol and cardiac heath where low-to-moderate consumption reduces the risk of CVDs by influencing coronary artery-associated events and improving anti-oxidant status, while long-term heavy intake causes myocardial structural damage and non-ischemic cardiomyopathy termed alcoholic cardiomyopathy (ACM) [1–3]. ACM is characterised by increased left ventricular mass, fibrosis, structural alterations, impaired

contractility, mitochondrial dysfunction, oxidative and nitrative stress, eventually leading to heart failure [4, 5]. Studies report that dose dependent effects of alcohol on the heart is mediated by the serine/threonine kinase AKT wherein *Akt* knockout induced cytotoxicity and cell death, counteracting the benefits of low levels of alcohol [6]. The phosphorylation and activation of AKT is controlled by PTEN phosphatase (Phosphatase and tensin homologue deleted on chromosome 10) by modulating PIP3 ((PI-3,4,5-triphosphate) levels within the cell. AKT can also modulate mitochondrial morphology [7] and the organelle's ultrastructural abnormalities [8, 9] promotes cardiomyocyte apoptosis during alcohol toxicity.

Mitochondria are dynamic subcellular organelles that continuously fuse and divide to meet the energy demands of the cell, ensure functional mitochondrial population and regulate apoptosis [10–12]. Fragmented mitochondria, frequently observed during apoptosis, can be a cause or result of apoptotic event. In mammalian cells, mitochondrial outer membrane (MOM) fusion is mediated by the mitofusins (MFN1/2), mitochondrial inner membrane (IMM) fusion by optic atrophy protein-1 (OPA1) and stomatin-like protein 2

✉ Ramasamy Subbiah
subbiahr@nrcbsmku.org

1   Cardiac Hypertrophy Laboratory, Department of Molecular Biology, School of Biological Sciences, Madurai Kamaraj University, Madurai 625 021, Tamil Nadu, India

(SLP2) while fission is facilitated by dynamin-related protein 1 (Drp1) and hFis1 [13]. Drp1 is a cytoplasmic GTPase that undergoes phosphorylation/dephosphorylation for its activation and translocation to the mitochondrial scission site [14, 15], while hFis1 is a resident MOM protein facing the cytoplasm [16]. Several cardiac diseases like hypertrophy, myocardial infarction, ischemia–reperfusion (I/R) injury and pressure-overload-induced heart failure are associated with elevated Drp1 levels and mitochondrial fragmentation, in which silencing or inhibition of the same confers cardioprotection. Expression of the dominant negative mutated form of Drp1 or pharmacological inhibition with Mdivi-1 (Mitochondrial division inhibitor-1) prevented mitochondrial permeability transition pore (MPTP) opening, reduced infarct size, calcium overload and reactive oxygen species (ROS) generation during I/R injury [17, 18]. It also prevented the development of pathological hypertrophy [19, 20] and improved insulin response to H_2O_2 cytotoxicity [21]. P110, a peptide that selectively inhibits the interaction between Drp1 and Fis1, also reduced infarct size, ROS generation and cytochrome c release during I/R injury [22]. Given that mitochondria are abundant in cardiomyocytes and produce ATP by oxidative phosphorylation for cardiac contractility, it is not surprising that mitochondrial structural integrity is important for cardiac functions.

Based on these previous studies, we hypothesised that inhibition of mitochondrial fission could improve myocardial functions during chronic alcohol exposure. Interestingly, Drp1 depleted cardiomyoblasts showed increased sensitivity to ethanol by promoting Bak-mediated MOMP for cytochrome c release and caused mitochondrial PTEN-L accumulation for interaction with MFN1 and organelle dysfunction. Inhibition of PTEN-L activity with VO-OHpic reverted the cytotoxicity of ethanol and reduced its accumulation in the mitochondria, both in vivo and in vitro, demonstrating that PTEN-L is directly involved in regulation of mitochondrial phase of apoptosis, in conditions where fission is a dispensable process. Furthermore, our study also provides in vivo evidence that global inhibition of PTEN activity with VO-OHpic has significant cardioprotective effects against ethanol induced myocardial toxicity.

Materials and methods

Materials

All tissue culture plates and flasks were obtained from Himedia Laboratories, India. Chemicals, reagents, siRNAs, primary and secondary antibodies purchased from Santa Cruz Biotechnology Inc., USA are as follows: MFN1 (sc-50330), MFN2 (sc-50331), Fis1 (sc-376447), GAPDH (sc-47724), VDAC1 (sc-8828), cytochrome c (sc-13156),

Akt1 (sc-5298), pAkt1 (Ser473) (sc-293125), goat anti-rabbit IgG-HRP conjugated secondary antibody (sc-2030), anti-mouse IgGK BP-HRP conjugated secondary antibody (sc-516102), VO–OHpic [Aqua (3-hydroxy-2-pyridinecarboxylato-kapaN1,kapaO2)[3-(hydroxy-kapaO)-2-pyridinecarboxylato(2-)-kapaO2]oxo-vanadate(1-), hydrogen, trihydrate] (sc-216061), N-Acetyl-Asp-Glu-Val-Asp p-nitroaniline (Ac-DEVD-pNA) (Cat.No.: sc-311275), *Drp1* siRNA (sc-43732), and scramble siRNA (sc-37007). Bak (Cat.No. #12105), Beta-Actin (Cat.No. #3700), OPA1 (Cat.No. #80471), Drp1 (Cat.No. #14647), Mff (Cat.No. #86668) and p-Drp1 (Ser616) (Cat.No. #3455) primary antibodies were purchased from Cell Signalling Technology Inc., USA, and SLP2 (PA-1-84301), MiD51 (Cat.No. 20164-1-AP) and MiD49 (Cat.No. 16143-1-AP) from Proteintech Group, USA. PTEN antibody (#245322) was purchased from Abcam, UK and Caspase-3 (PA5-16335) from Thermofisher Scientific, USA. Protease inhibitor cocktail (Cat. No. P8340) from Sigma-Aldrich Inc., USA was used for protein isolation protocols. Lipofectamine RNAiMAX Transfection Reagent (Cat.No. #13778-075) was purchased from Invitrogen Inc., USA and Resveratrol (Cat.No. 02196052) was purchased from MP Biomedicals, USA.

In vivo treatment protocol

Internal Research and Review Board, Ethical Clearance, Biosafety and Animal Welfare Committee of Madurai Kamaraj University, in accordance with NIH Guidelines, approved all animal experiments and procedures for care and use of laboratory animals. Wistar albino rats were housed and maintained in animal house with 12 h day/night cycle, at 25ºC and fed with standard rat chow (Hindustan Lever Limited, India) and deionised water, ad libitum.

Ethanol treatment protocol

Female Wistar rats of 180–210 g body weight was used for this study and alcohol treatment was given as per protocol by Pushpakiran et al. (2004) with modifications [23]. Animals were randomly selected and categorised into two groups: Group I: Control (n = 6), and Group II: Ethanol treatment (n = 6). Animals of EtOH group received 5 g/kg body weight of ethanol orally via gavage, daily, for 9 weeks. The dose was gradually increased from 0.5 g to 5 g of ethanol over a period of 20 days for adaptation and then maintained for 9 weeks at 5 g/kg body weight. Control animals were given sucrose calorically balanced with that of ethanol, orally, via gavage for the treatment period. Periodical body weight measurement was performed. On the last day, animals were fasted for 12 h, body weight recorded and anaesthetised with ketamine (100 mg/kg body weight). Blood was collected by cardiac puncture and heart tissue was harvested,

perfused in sterile phosphate buffered saline (1X: 137 mM NaCl, 2.7 mM KCl, 4.3 mM Na_2HPO_4, 1.47 mM KH_2PO_4, pH 7.4) and stored at -80°C.

VO–OHpic treatment protocol

To evaluate the therapeutic potential of VO–OHpic for chronic alcohol consumption induced organ damage, the following protocol was performed: Female Wistar rats of 180-210 g body weight was used for this study and alcohol treatment was given as mentioned previously. Animals were randomly selected and categorised into four groups: Group I: Control (CON), Group II: Ethanol-treatment (EtOH), Group III: VO–OHpic treatment only (VO–CON), Group IV: VO–OHpic + EtOH treatment (VO–EtOH). For the VO–OHpic treatment, a dose of 10 µg/kg body weight was given by intraperitoneal injection, once every three days, 30 min prior to ethanol treatment [24]. Periodical body weight measurement was performed and the treatment was maintained for 9 weeks before harvesting of organs.

Histological assessment

For histological examination of tissue sections, 10% formaldehyde fixed heart tissues were paraffin embedded by standard protocols [25]. 5 µm thin sections were made, dehydrated, stained with Hematoxylin & Eosin (H&E) and observed under × 40 objective of light microscope (Nikon, Japan). The images were analysed with the help of a qualified pathologist blinded to the treatment conditions and quantified with Image J software (https://imagej.nih.gov/ij/).

Estimation of serum biochemical parameters

Serum was isolated from blood samples by centrifugation at 2000 rpm for 10 min at 4 °C and estimated for Creatine Kinase-MB (CK-MB) as per manufacturer's protocol (Siemens, USA).

Tissue homogenate preparation

100 mg of heart tissue was homogenised in lysis buffer (20 mM Tris–HCl, pH 7.5, 150 mM NaCl, 1 mM Na_2EDTA, 1% Triton X-100, 1% sodium deoxycholate, 1 mM Na_3VO_4) supplemented with protease inhibitor cocktail. Following incubation of the homogenate on ice for 20 min, it was centrifuged at centrifugation at 12500 rpm, 15 min, 4°C and supernatant collected. Aliquots of the supernatant were made and stored at -80°C.

Estimation of protein concentration

Protein concentration was estimated by Bradford assay [26] with Bradford reagent (Sigma-Aldrich Inc., USA). Bovine Serum Albumin (BSA) was used as standard.

Estimation of cardiac malondialdehyde (MDA) concentration

Induction of oxidative stress in total heart homogenate/cell lysate was analysed with lipid peroxidation assay following TBARS (thiobarbituric acid-reactive substances) method [27] with 1,1,3,3′-tetramethoxy-propane (TMP) as standard. 200 µL of 10% TCA was added with 100µL of tissue homogenate for protein precipitation and kept in ice for 15 min. The samples were centrifuged at 2500 rpm, 15 min, 4°C. Equal volume of 0.67% Thiobarbituric acid (TBA) was added to 200 µL of supernatant and incubated in boiling water bath for 10 min. TMP was also processed the same way and the colour developed was read at 532 nm.

Estimation of total antioxidant levels

Total antioxidant level was estimated with Antioxidant Assay Kit (Sigma-Aldrich Inc, USA) as per manufacturer protocol. The assay is based on the formation of ferryl myoglobin radical from metmyoglobin and hydrogen peroxide, that oxidises ABTS (2,2′-azino-bis (3-ethylbenzthiazoline-6-sulfonic acid) to ABTS$^{·+}$ cationic radical, a green coloured chromogen. The concentration was measured spectrophotometrically at 405 nm. Trolox, a vitamin E analog, is used as standard and data is represented as Trolox Equivalence Capacity (mM).

Cell culture

Rat embryonic cardiomyoblast-derived H9c2 cells (purchased from National Centre for Cell Science, Pune, India) were grown and maintained in Dulbecco's Modified Eagle's Medium (DMEM) (Lonza, Belgium) supplemented with 10% Fetal Bovine Serum (Gibco, Grand Island, NY), 100U/ml of penicillin and 100 µg/ml streptomycin at 37 °C, 5% CO_2.

To study ethanol-induced cytotoxicity, cells were treated with 100 mM ethanol for 48 h and ethanol containing media was changed at 24 h [28].

Alcohol induced oxidative stress was defined by pre-treatment with Resveratrol (RES) at 200 nM for 4 h followed by ethanol treatment for 48 h, as per protocol mentioned above. To define the role of PTEN during alcohol-induced cytotoxicity, VO–OHpic was used as pre-treatment at a dose of 300 nM for 20 min [29]. Culture medium was changed, and cells were then exposed to ethanol.

Pharmacological inhibition of Drp1 is studied with pre-treating H9c2 cardiomyoblasts with Mdivi-1 (sc-215291, Santa Cruz Biotechnology, USA) at a dose of 5 µM for 30 min followed by ethanol treatment [30].

siRNA transfection

siRNA directed against *Drp1* and scramble siRNA were transfected using Lipofectamine RNAiMAX. H9c2 cells were grown to 50–60% confluency and transfected with Drp1 siRNA or scramble siRNA (Scr.siR) as per manufacturer protocol. Culture medium was changed after 6 h and cells allowed to grow for 24 h prior to ethanol treatment protocol. Knockdown efficiency was validated using Western blot with protein specific antibody.

Cell viability assay

Cell viability was measured by MTT Assay. The assay is based on the reduction of 3-(4,5-dimethylthiazol-2-yl)-2,5-diphenyltetrazolium bromide (MTT) (Cat.No.:M2003, Sigma-Aldrich Inc., USA) by active mitochondrial population to produce water-insoluble formazan crystals. To assess ethanol induced cytotoxicity, equal number of cells were plated in 96-well plates and incubated with 100 mM of ethanol for 48 h at 37 °C, with ethanol containing media changed at 24 h. MTT, at a final concentration of 0.5 mg/ml, was added to cells and incubated for 4 h at 37ºC following completion of treatment protocol. Cells were washed with $1 \times$ PBS and the formazan crystals formed were dissolved with 100 µL of DMSO. Absorbance was read at 570 nm with a microplate reader. Cells incubated with control medium were considered 100% viable. Data are represented as percentage relative viability, from experiments performed three times.

Cellular staining

Mitochondrial structure was analysed by culturing and treating H9C2 cells with EtOH in the above-mentioned protocol and stained with MitoTracker Green (Molecular Probes USA) to a final concentration of 50 nM in culture media and incubated for 30 min at room temperature (RT). Cells were washed with PBS and imaged with fluorescent microscope. Prolong Diamond Antifade Mountant DAPI (Molecular Probes, USA) was used to stain the nucleus.

Mitochondrial membrane potential changes were estimated using TMRE dye on equal number of cultured cells. After appropriate treatment, the cells were incubated with 20 nM TMRE dye for 30 min at 37 °C. After washing, the plate was measured using fluorescence compatible plate reader at Ex/Em of 530/580 nm. FCCP was used as positive control for the experiment.

Ethanol induced superoxide production was estimated by incubating cells with 2.5 µM final concentration of Mito-SOX Red (Molecular Probes, USA) in dark for 15 min, at 37 °C. Cells were washed with PBS and imaged with fluorescent microscope. Fluorescence is normalised to control group and four to five fields per samples were analysed.

Estimation of ATP levels

Cellular ATP levels were measured as per manufacturer's protocol with ATP Bioluminescent Assay Kit (Cat.No.: K254-200, BioVision Inc., USA). Briefly, 1×10^4 cells were seeded in 96-well plates and exposed to different treatment conditions. 100µL of nuclease releasing buffer was added to the cells and incubated for 5 min with gentle shaking followed by addition of 10µL of ATP monitoring enzyme. Luminescence was read immediately with luminometer (Tecan Group, Switzerland).

Isolation of mitochondrial fraction

For isolation of crude mitochondrial fraction from heart tissues, the protocol by Gostimskaya and Galin (2010) was followed [31] and isolation from appropriately treated cells was performed according to protocol by Frezza et al. [32].

Western blotting

Protein was isolated from heart tissue or harvested cells with lysis buffer supplemented with protease inhibitor cocktail, as mentioned previously. Equal quantities of protein samples were separated on SDS–polyacrylamide gel electrophoresis and electro-transferred onto PVDF membranes (Millipore, USA) following standard protocols. The membranes were blocked with 5% BSA prepared in Tris-buffered saline (pH 7.2) containing 0.1% Tween-20 (TBST) for 30 min and incubated with primary antibody, overnight, at 4 ºC: Drp1 (1:1000), p-Drp1 (Ser616) (1:800), Fis1 (1:1000), Mff (1:2000), MiD51 (1:1500); MiD49 (1:1500), Caspase-3 (1:1500), MFN1 (1:1000), MFN2 (1:1000), OPA1 (1:800), SLP2 (1:2000), AKT1 (1:1000), pAKT1 (1:1000), PTEN (1:1000), cytochrome c (1:800), Bak (1:1500). Subsequently, the membranes were washed thrice with TBST for 15 min each and incubated with appropriate secondary antibody conjugated to HRP for 1 h at RT. The membranes were developed with enhanced chemiluminescence and quantified with ImageJ software. GAPDH (1:1000) and Beta-Actin (1:1000) were used as loading controls for total and cytoplasmic proteins and VDAC (1:1000) for mitochondrial fractions.

RNA Isolation, cDNA synthesis and qRT-PCR

Total RNA was isolated from appropriately treated and control cells using Tri Reagent (Sigma-Aldrich Inc. USA). cDNA construction and *q*RT-PCR were performed as per protocol by Rekha et al. [33]. The primers used for cytochrome *c* and internal control GAPDH are the following [34]: Cyt.c Forward Primer: 5′GCCCAGTGCCAC ACTGT3′; Reverse Primer: 5′CTGTCTTCCGCCCGAACA 3′; GAPDH Forward Primer: 5′CTGAGAATGGGAAGC AGGTC3′; Reverse Primer: 5′GAAGGGGCAGAGATG ATGAC3'.

Co-immunoprecipitation

For co-immunoprecipitation experiments, 1 mg of protein samples from heart tissue samples of the four group of animals were used. Co-immunoprecipitation was performed as per manufacturer protocol from Crosslink Immunoprecipitation Kit (ThermoScientific, USA) and eluted proteins were processed and stored in SDS-sample buffer for western blotting experiments. Anti-rabbit secondary antibody (of IgG) was also prepared and processed the same as above mentioned protocol and used as negative control for the experiments.

Statistical analysis

Statistical analysis was performed with GraphPad Prism, version 6.0 and data are represented as mean±standard error of mean (SEM). Statistical significance (P-value) is calculated with unpaired Student's *t* test for comparison between two groups and one-way ANOVA followed by Bonferroni correction for comparison among three or more groups. No data points were excluded from the analysis and P<0.05 was considered statistically significant.

Results

Chronic alcohol ingestion induces cardiac hypertrophy, in vivo, with increased mitochondrial fission.

Animals ingesting ethanol for a period of 9 weeks did not show any significant difference in body weight compared to control, but tissue damage markers, like LDH, AST and ALT were significantly elevated during ethanol ingestion (data not shown). Elevated serum CK-MB levels is most commonly used as a predictor of myocardial damage and chronic alcohol ingested animals showed slightly increased serum CK-MB levels compared to control (Supplementary Fig. 1A). These animals also displayed significantly

increased heart weight/ body weight ratio (Fig. 1a) and heart tissue sections showed hypertrophy of the cardiomyocytes along with mild inflammatory response (Fig. 1b, 1c) compared to pair-fed control.

Oxidative stress is one of the prime modes of cardiotoxicity during chronic alcohol consumption. A state of oxidative stress is caused when the ratio of ROS to antioxidants is elevated, thus damaging DNA, proteins and lipids. Lipid peroxidation of hearts increased in ethanol-ingested animals compared to pair-fed controls (Supplementary Fig. 1B) but there was no significant difference in the total antioxidant levels between the two groups (Supplementary Fig. 1C). Mitochondria are both the source and target of ROS and its fusion-fission dynamics ensure functional mitochondrial population. Oxidative stress prompts mitochondrial fragmentation [35] leading to cellular death. Analysis of mitochondrial fission associated proteins in heart tissues of chronic alcohol ingested animals showed no statistical difference in total Drp1 levels between control and ethanol treated animals, but pDrp1 (Ser616) was significantly increased upon ethanol treatment (Fig. 1d, e). Other mitochondrial fission associated proteins that act as receptors for Drp1 on the mitochondria, like hFis1, Mff and MiD41 did not show significant difference between control and ethanol treated animals but MiD51 was significantly downregulated in ethanol treated animals compared to control animals (Fig. 1d, f, g). Similar expression was observed in H9c2 cells, where ethanol significantly increased pDrp1 levels compared to control (Fig. 1h, i). Together, these results demonstrate that chronic exposure of alcohol induces oxidative stress and alters mitochondrial structural homeostasis towards fragmentation by increasing the expression of fission protein, Drp1, in vivo and in vitro.

Silencing of *Drp1* aggravates alcohol-induced mitochondrial dysfunction, in vitro

To evaluate the role of mitochondrial fission in alcohol-induced toxicity, *Drp1* silenced H9c2 cells were exposed to ethanol and analysed for cytotoxicity and apoptosis. Surprisingly, silencing of *Drp1* in cardiomyoblasts (Fig. 2a, b) decreased cell viability during ethanol exposure compared to scramble siR control cells (Fig. 2c), but it was still significantly higher than scramble siR transfected EtOH-treated cells. EtOH exaggerated superoxide production in Drp1 depleted cardiomyoblasts compared to scramble siR transfected cells (Fig. 2d, e), but did not significantly alter mitochondrial membrane potential in both scramble and *Drp1* silenced sets (Fig. 2f). Consistent with this, *Drp1* silenced cells displayed increased lipid peroxidation (Supplementary Fig. 2a) and depressed antioxidant levels (Supplementary Fig. 2B) during ethanol treatment compared to scramble control, but there was no significant difference in antioxidant
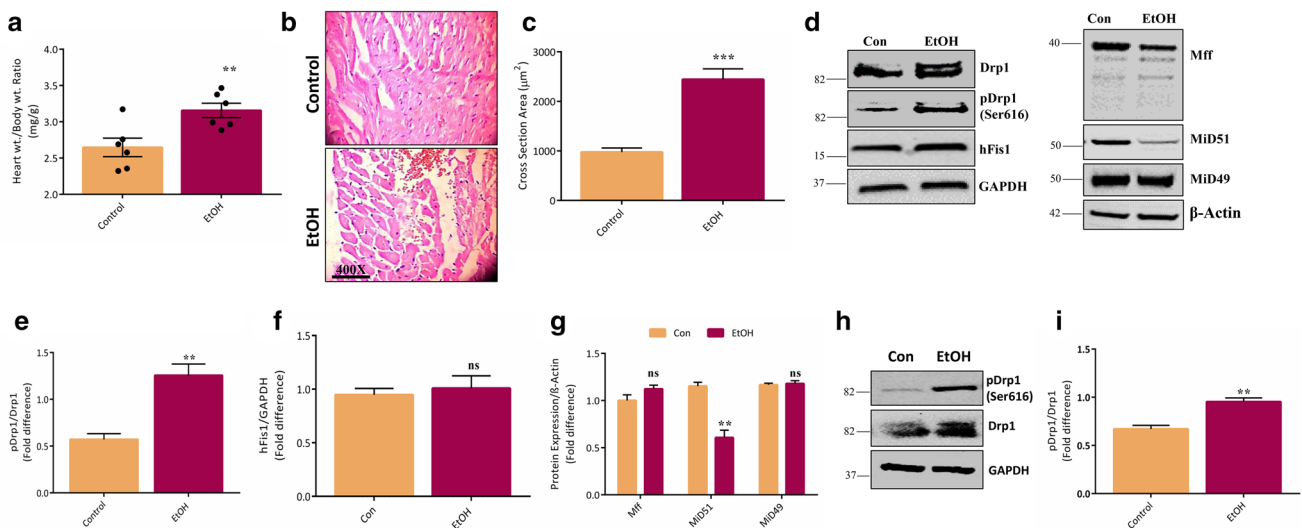
Fig. 1 Chronic alcohol exposure induced cardiac hypertrophic response and increased Drp1 expression, in vivo and in vitro. **a** Heart/body weight ratio (mg/g) increased in animals consuming ethanol (n = 6). **b** Representative images of histological examination of control (Con) and ethanol treated (EtOH) heart sections stained with H&E. **c** Quantitation of cross-sectional area of cardiomyocytes (μm^2) in histology sections. **d** Western blot showing increased expression of Drp1, decreased MiD51 and no difference in hFis1, Mff, MiD49 levels, in ethanol treated animals. **e** Quantitative representation of pDrp1/Drp1 levels in control and ethanol treated hearts, normalised to expression levels of GAPDH. **f** Quantitative representation of hFis1 levels between control and ethanol treated animals, normalised to GAPDH. **g** Quantitative representation of Mff, MiD51 and Mid49 between control and ethanol treated, normalised to β-Actin. **h** Western blot of H9c2 cells exposed to ethanol showing increased expression of pDrp1(Ser616). **i** Quantitative representation of western blot of pDrp1/Drp1 levels in H9c2 cells. Statistical significance was determined via Student's *t* test and data are represented as mean ± SEM where ***P < 0.001, **P < 0.01, *ns* no significance versus the control group

levels between ethanol treated cells of both sets. In addition, while ethanol treatment significantly increased ATP levels in scramble and Drp1 depleted cells, it was significantly lower in *Drp1* silenced cells treated with ethanol compared to scramble ethanol treated cells (Fig. 2g). Alcohol-induced changes in ATP levels is a tissue specific response [36, 37] and the increased ATP levels observed could be an initial adaptive response to ethanol insult.

Mitochondria are central to apoptosis regulation by internalising pro-apoptotic proteins like cytochrome c that can trigger the activation of caspases. Sequestering these proteins within its membranes depend on the structural integrity [38–41]. Because tubular mitochondria are frequently observed during silencing of *Drp1*, ethanol-induced expression changes in the fusion proteins (MFN1/2, OPA1 and SLP2) were analysed in crude mitochondrial fraction. Ethanol treatment increased the expression of MFN1 in both scramble and *Drp1* siRNA transfected cells compared to scramble control cells but was not significantly different between the two treated groups. MFN2 was significantly downregulated in both scramble and Drp1 depleted cells upon ethanol treatment and was significantly lesser in *Drp1* silenced cells compared to scramble EtOH cells (Fig. 3a, b). On analysing for OPA1 and SLP-2, ethanol supressed expression of both in scramble-siRNA transfected cells (Fig. 3a, b). While *Drp1* silencing restored SLP-2 levels

upon ethanol treatment, OPA1 remained supressed (Fig. 3a, b). In addition to its fusion function, OPA1 also maintains cristae structure to retain the pro-apoptotic proteins. This supressed OPA1 expression in ethanol treated Drp1 depleted cells correlated with cleavage and activation of caspase-3 (Fig. 3c, d). To analyse whether apoptosis or other cell death mechanisms are in play, *Drp1* silenced cells were pre-treated with z-vad-fmk (a pan-caspase inhibitor) exposed to ethanol and analysed for cell viability. We observed that the presence of caspase inhibitor protected the cells and improved survival in both scramble siR and *Drp1* siR transfected cells treated with ethanol (Supplementary Fig. 2C). Therefore, ethanol exposure worsened mitochondrial dysfunction by impairing fusion machinery and increasing superoxide production for apoptosis in *Drp1* silenced cells.

Resveratrol abrogated ethanol potentiated $O_2^{\cdot-}$ production in Drp1 depleted cardiomyoblasts

Excess mitochondrial superoxide generation observed in Drp1 depleted cardiomyocytes on exposure to ethanol indicate that oxidative stress could be the cause of ensuing defects. To validate this, cells were pre-treated with resveratrol (RES), a potent antioxidant that improves cardiac functions by activating cell survival pathways, mitophagy
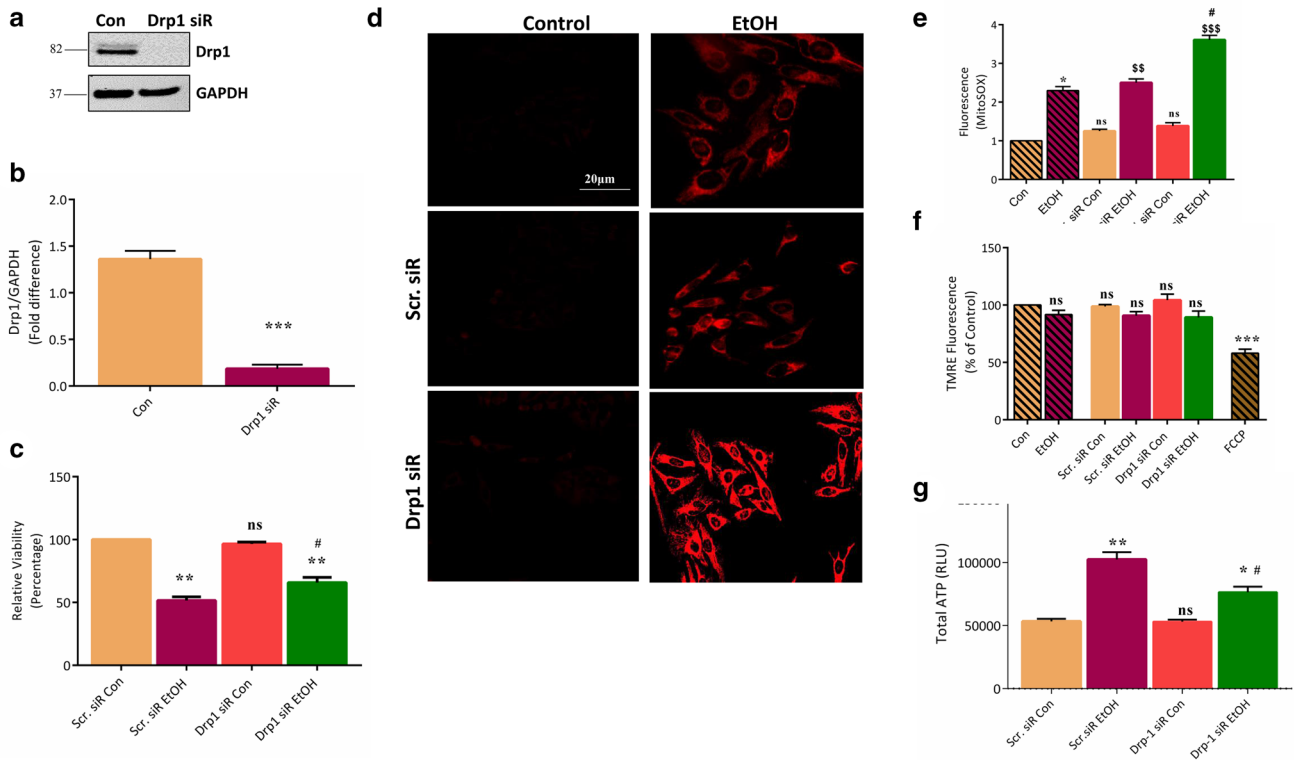
Fig. 2 Silencing of *Drp1* did not confer protection to H9c2 cells treated with ethanol. **a** Western blot confirming silencing of *Drp1* on transfection of H9c2 cells with *Drp1* siRNA. **b** Quantitative representation of *Drp1* silencing in **a**. **c** Depleting H9c2 of Drp1 reduced cell viability on ethanol exposure. **d** Ethanol exaggerated mitochondrial superoxide production during Drp1 depletion as detected with MitoSOX Red. **e** Quantification of relative MitoSOX Red fluorescence levels between scramble and Drp1 depleted cells. **f** Ethanol did not alter mitochondrial membrane potential in both scramble and

Drp1 silenced cells. **g** Total ATP levels are depleted in *Drp1* silenced cells on ethanol treatment. Statistical significance was determined with student's *t* test and one-way ANOVA and data are represented as Mean ± SEM where ***$P < 0.001$, **$P < 0.01$, *$P < 0.05$, *ns* not significant versus the control group (CON), $^{\$\$\$}P < 0.001$, $^{\$\$}P < 0.01$, $^{\$}P < 0.05$, *ns* not significant versus scramble siRNA transfected (Scr. siR Con) and $^{\#\#}P < 0.01$, $^{\#}P < 0.05$ versus ethanol treated group (EtOH)

of dysfunctional mitochondria, mitochondrial biogenesis and expression of antioxidant genes [42–45].

RES pre-treatment improved viability of Drp1 depleted cardiomyoblasts exposed to ethanol almost equivalent to that of non-RES treated control cells with significant improvement in cell viability in both scramble and *Drp1* silenced cells exposed to ethanol compared to EtOH-only treated cells (Fig. 4a). Both Drp1 depleted and scramble cells displayed significantly supressed levels of mitochondrial superoxide during RES + EtOH compared to scramble EtOH not pre-treated with RES (Supplementary Fig. 3, Fig. 4b). RES also significantly decreased lipid peroxidation during ethanol treatment in both scramble and *Drp1* siRNA transfected cells compared to both control and EtOH-only treated cells (Fig. 4c). RES treatment did not change ATP levels in scramble and Drp1 depleted cells compared to RES-untreated control cells and prevented the adaptive increase in its levels in scramble EtOH treated cells (Fig. 4d). Overall, these data establish that

ethanol-promoted oxidative stress induces the observed cytotoxic effects when *Drp1* is silenced in H9c2 cells.

Mitochondrial PTEN-L dictates organelle dysfunction in Drp1 depleted cardiomyoblasts

Cellular stress signals activate several effector molecules like AKT to combat the ensuing oxidative stress which in turn can phosphorylate and activate targets for myocardial cell growth, metabolism, survival and contractility [46, 47]. Since ethanol exposure induced oxidative stress during Drp1 depletion in cardiomyoblasts, and the PTEN/PI3K/AKT pathway responds in a protective capacity to oxidative stress, the protein expression profile of PTEN, AKT1 and activated form of AKT1 (pAKT1-Ser473) were analysed. There was no significant difference in total AKT1 between scramble and *Drp1* silenced cells but ethanol treatment downregulated pAKT1 levels in Drp1 depleted cells only and not in scramble EtOH (Fig. 5a, b). Consistent with this, we observed an
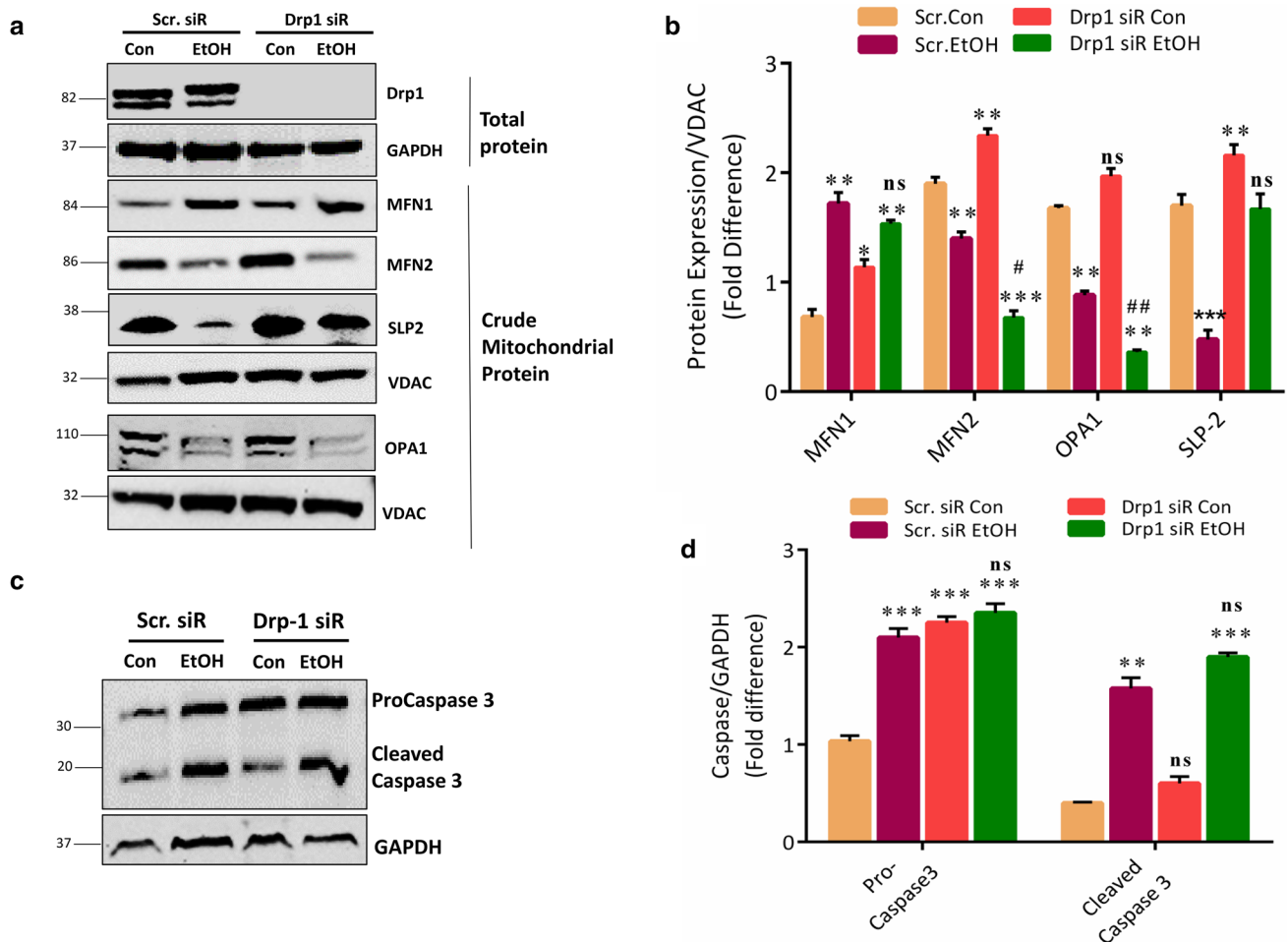
Fig. 3 Ethanol impairs mitochondrial fusion machinery for apoptosis in Drp1 depleted cells. **a** Immunoblot showing dysregulated mitochondrial fusion machinery in Drp1 depleted cells treated with ethanol. **b** Quantification of fusion proteins expression profile normalised to VDAC. **c** Immunoblot demonstrating activation of Caspase-3 for apoptosis during ethanol treatment in *Drp1* silenced cells. **d** Quantification of pro-caspase 3 and active caspase 3 levels in **c**, normalised to GAPDH. Statistical significance was determined by one-way ANOVA and data are represented as mean ± SEM where ***$P < 0.001$, **$P < 0.01$, *$P < 0.05$, *ns* not significant versus the scramble control group (Scr. siR Con) and #$P < 0.05$, ##$P < 0.005$; ###$P < 0.001$; *ns* not significant versus scramble ethanol treated group (Scr. siR EtOH)

increase in PTEN expression in *Drp1* silenced cells treated with ethanol compared to scramble control while there was no significant change in its expression levels between the scramble untreated and treated cells (Fig. 5a, c). Interestingly, we also observed increase in the 70 kDa isoform of PTEN, PTEN-L, a secretory variant that regulates signalling in neighbouring cells [48]. Ethanol treatment increased PTEN-L expression in both scramble and *Drp1* silenced cells compared to control cells with a significantly higher level in Drp1 siR EtOH (Fig. 5a, c).

Considering that PTEN-L localises to the mitochondria and we observed dysfunction of the organelle during both ethanol treatment and *Drp1* silencing, we sought to understand the interlink between the two. For this, PTEN was inhibited by two approaches: (1) pharmacological

inhibition of activity with VO–OHpic (VO) and (2) siRNA targeted to *PTEN*. VO is a water-soluble vanadium complex that reversibly inhibits PTEN and promotes insulin-like effects at nanomolar concentration [29]. To confirm the inhibitory activity of VO on PTEN, we looked for increment in pAkt levels as an indirect measure and for its effect on PTEN-L, we analysed its mitochondrial accumulation upon ethanol treatment. Pre-treatment with VO–OHpic significantly increased the levels of pAKT1 (Ser473) compared to untreated control at 20 min and then reverted to that of control at 24 h and 48 h (Supplementary Fig. 4A, Supplementary Fig. 4B). Ethanol-induced mitochondrial PTEN-L accumulation was significantly reduced in VO pre-treated cells (Fig. 5d, e) confirming that 20mins pre-treatment was enough to exert its effect. This
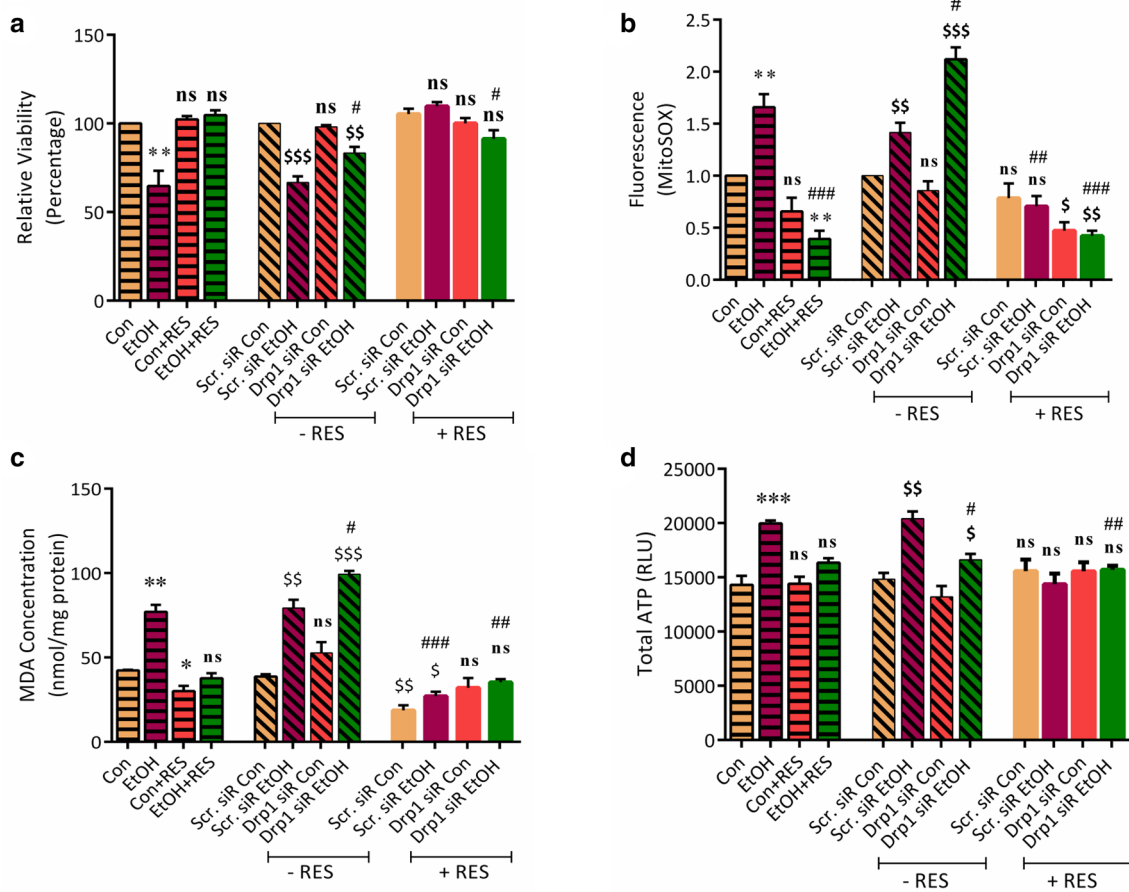
Fig. 4 Oxidative stress facilitates ethanol-induced mitochondrial dysfunction during Drp1 knockdown. **a** Ethanol-potentiated loss in cell viability is abrogated by pre-treatment with RES in Drp1 depleted cells. **b** Quantitative representation of relative fluorescence of MitoSOX shows RES treatment reduced mitochondrial superoxide production during inhibition of Drp1. **c** Pre-treatment with RES reduced lipid peroxidation of *Drp1* silenced cells treated with ethanol. **d** Ethanol treatment increased total cellular ATP levels in Drp1 depleted cells. Statistical significance was determined with one-way ANOVA and data are represented as mean ± SEM where ***$P < 0.001$, **$P < 0.01$, *$P < 0.05$, *ns* not significant versus the control group (Con), $^{\$\$\$}P < 0.001$, $^{\$\$}P < 0.01$, $^{\$}P < 0.05$, *ns* not significant versus scramble control cells that were not pre-treated with RES and $^{\#\#\#}P < 0.001$, $^{\#\#}P < 0.01$, $^{\#}P < 0.05$, *ns* not significant versus scramble ethanol treated cells that were not pre-treated with RES

was used in subsequent Drp1 knockdown experiments. We also observed sustained upregulation of pDrp1 levels upon ethanol treatment, irrespective of VO treatment (Fig. 5d, e).

We detected significantly lower levels of PTEN-L in Drp1 knockdown cells upon pre-treatment with VO, in both ethanol treated and untreated cells, compared to VO untreated set (Fig. 5f, g). These cells also demonstrated increased cell viability compared to VO-untreated *Drp1* knockdown conditions (Fig. 5h) and despite an increase in pro-caspase 3 levels in *Drp1* silenced cells, VO pre-treatment prevented its cleavage and activation (Fig. 5i, j). VO treatment also prevented EtOH-induced increase in ATP levels in both scramble and Drp1 depleted cells compared to EtOH-only treated cells (Supplementary Fig. 4C) along with supressing mitochondrial superoxide levels (Supplementary Fig. 4D, E)

and lipid peroxidation of *Drp1* silenced cells treated with ethanol (Supplementary Fig. 4F).

To substantiate that these results are: (1) restricted to PTEN phosphatase activity, *PTEN* silenced H9c2 were analysed and showed significantly lower cell viability, even without ethanol treatment (data now shown); (2) not restricted to knockdown of *Drp1*, cells were pre-treated with Mdivi1 followed by ethanol exposure. These cells sustained the loss in cell viability (Supplementary Fig. 5A), increased lipid peroxidation (Supplementary Fig. 5B), showed no significant difference in supressed antioxidant levels with EtOH-only treated cells (Supplementary Fig. 5C) and significantly reduced ATP levels compared to both control and EtOH treated cells (Supplementary Fig. 5D).

Overall, these results provide evidence that mitochondrial fission could be dispensable for ethanol-mediated
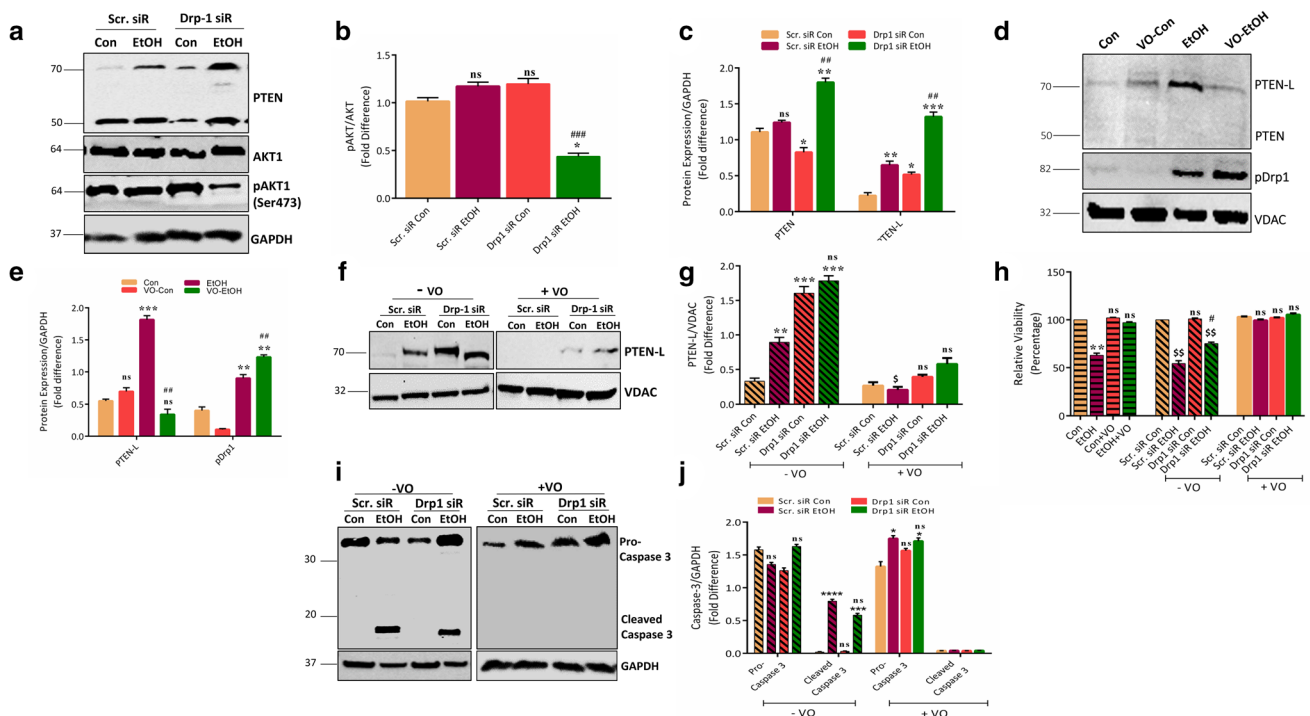
Fig. 5 PTEN phosphatase regulates mitochondrial functional status during *Drp1* silencing in H9c2 cells. **a** Ethanol treatment increased PTEN-L expression in *Drp1* silenced cells. **b** Quantification showing supressed activation of Akt in Drp1 depleted cells treated with ethanol. **c** Quantification of PTEN and PTEN-L levels normalised to GAPDH. **d** VO (300 nM for 20mins) treatment prevented mitochondrial PTEN-L accumulation and did not influence pDrp1 levels. **e** Quantification of western blot data in **d**. **f** VO prevents mitochondrial PTEN-L accumulation in Drp1 knockdown cells, treated with and without ethanol. **g** Quantification of western blot in **f**, normalised to VDAC. **h** VO improves cell viability in Drp1 knockdown cells treated with ethanol. **i** Caspase 3 activation is prevented upon VO pre-treatment to Drp1 silenced cells treated with ethanol. **j** Quantification of caspase-3 levels in **i**. Statistical significance was determined with one-way ANOVA and data are represented as mean ± SEM where ***P < 0.001, **P < 0.01, *P < 0.05, *ns* not significant versus respective control group, $$P < 0.01, $P < 0.05 versus scramble control and ##P < 0.01, #P < 0.05, *ns* not significant versus scramble ethanol treated group

cytotoxicity as cell death occurs even in the absence of Drp1, the major fission protein, and that PTEN-L has a potential role to play in promoting mitochondrial dysfunction.

PTEN-L is required for Bak-mediated MOMP and cytochrome c release in Drp1 depleted cardiomyoblasts during ethanol exposure

In response to cell death stimuli, cytoplasmic BH3-only proteins (PUMA, BID, Bim, Bad, Noxa, Bik) interact with Bax/Bak to induce their conformational change and accumulate in MOM to form pores/channels [49]. These pores act as a gateway for the release of cytochrome c and other apoptotic factors within the mitochondrial membranes. Research by Estaquier and Arnoult [50] and Parone et al. [51] report that during Bax/Bak mediated MOMP, inhibition of mitochondrial fission delayed, but did not completely prevent, the release of cytochrome c. Also, Madesh et al., show that superoxides facilitate alcohol-induced hepatotoxicity by

inducing Bak-, not Bax-, dependent MOMP and mitochondrial dysfunction [52].

Our study also showed significantly increased Bak levels in the mitochondrial fraction of both scramble and Drp1 depleted cells treated with ethanol compared to untreated scramble control (Fig. 6a, b). While Bak levels in *Drp1* knockdown cells was significantly lower than that seen in scramble siRNA transfected cells treated with ethanol, it was still significantly higher than scramble control. VO pre-treatment prevented mitochondrial Bak accumulation upon ethanol treatment and Drp1 knockdown (Fig. 6a, b) and in turn significantly reduced the release of cytochrome c from the mitochondria to the cytoplasm when compared to VO-untreated cells (Fig. 6a, c). It should be noted that in VO-untreated cells, although Drp1 depletion caused significantly more cytochrome c to be retained within the mitochondria compared to scramble-ethanol cells, the release to the cytoplasmic fraction was still significantly higher in these cells. To understand the reason for this, we analysed the mRNA levels of cytochrome c and observed significantly
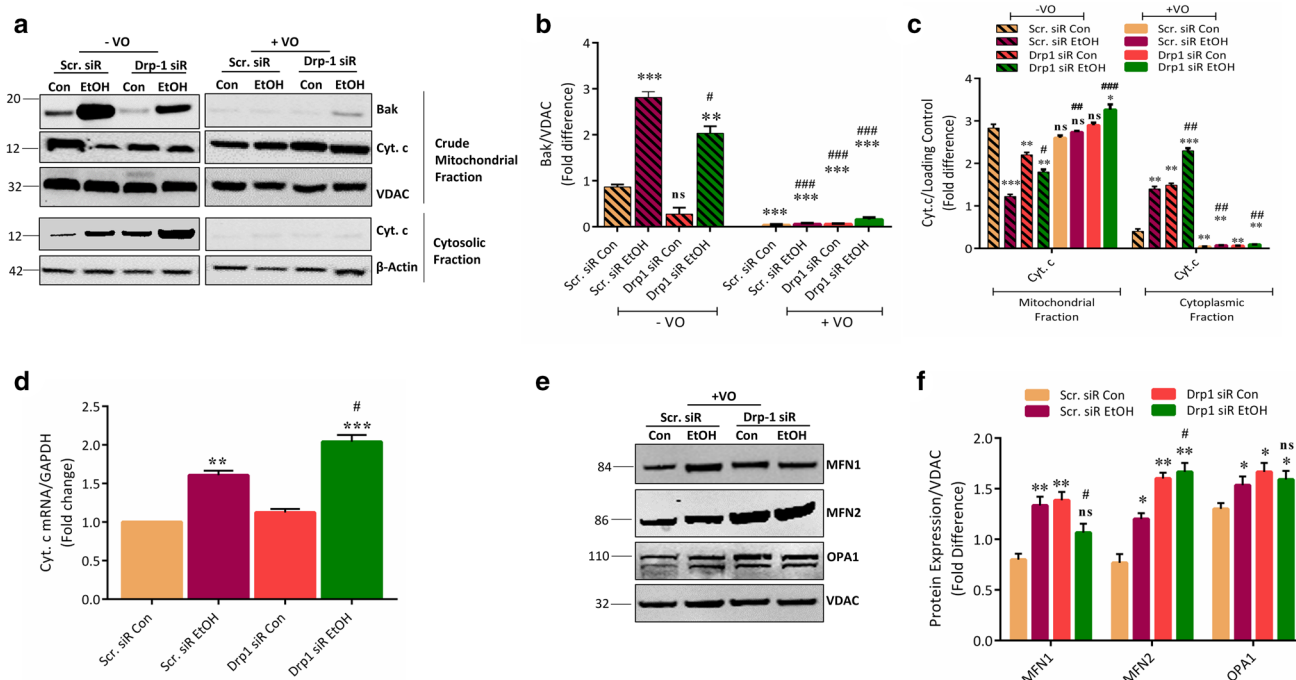
Fig. 6 Inhibition of PTEN phosphatase prevents Bak-mediated MOMP in Drp1 depleted H9c2 cells. **a** VO treatment prevented mitochondrial Bak accumulation and cytochrome c release in Drp1 knockdown cells. **b, c** Quantitation of western blot images in **a**. **d** Increased mRNA levels of cytochrome c upon ethanol treatment in *Drp1* silenced cells. **e** Expression profile of mitochondrial fusion proteins upon VO treatment in *Drp1* knockdown cells. **f** Quantitation of western blot images in **e**. Satistical significance was determined with one-way ANOVA and data are represented as mean ± SEM where ***P < 0.001, **P < 0.01, *P < 0.05, *ns* not significant versus respective control group and ##P < 0.01, #P < 0.05, *ns* not significant versus scramble ethanol treated group

upregulated mRNA levels in *Drp1* silenced cells treated with ethanol compared to scramble control and ethanol exposed cells (Fig. 6d).

Because Bax/Bak interacts with mitofusins on the mitochondrial membrane and changes association from MFN2 to MFN1 upon apoptosis stimulus [53], we next sought to analyse the effect of VO, and thus PTEN-L, in mitochondrial fusion. VO reverted MFN2 and OPA1 levels to that of control with a significant increase in MFN2 levels in *Drp1* silenced cells, treated with or without ethanol. While VO did not alter MFN1 levels between untreated and treated scramble and *Drp1* knockdown cells, it was significantly upregulated in scramble ethanol treated cells. All these data together demonstrate that stress conditions like ethanol and *Drp1* knockdown cause accumulation of PTEN-L on the mitochondria and that its localisation on the organelle's membrane is required for Bak mediated cytochrome c release.

PTEN-L-MFN1 interaction is required for alcohol-induced cardiotoxicity, in vivo and in vitro

To demonstrate that the effect of PTEN-L on mitochondrial dysfunction is not restricted to H9c2 cardiomyoblasts and

that its mitochondrial localisation is essential for apoptosis signals, we performed in vivo studies where animals were pre-treated with VO–OHpic and then maintained in ethanol treatment protocol. Inhibitory activity of VO was confirmed with increase in pAKT1 (Ser473) levels in heart tissues of VO-treated animals (Fig. 7a, b). Consistent with our in vitro experiments, VO prevented mitochondrial PTEN-L and Bak accumulation upon ethanol treatment (Fig. 7c, d) and showed sustained increase in pDrp1 levels (Fig. 7e, f). VO treatment significantly improved MFN2 and OPA1 levels in ethanol treated animals and normalised the upregulated MFN1 expression to that of control (Fig. 7g, h). To elucidate the relationship between PTEN-L and MFN1 for mitochondrial dysfunction, heart tissues from all the groups of animals were immunoprecipitated with MFN1 antibody and probed for complexed PTEN-L. We detected PTEN-L in EtOH consuming animals only and not in control or VO pre-treated animals (Fig. 7i) confirming that stressed hearts, like that during ethanol toxicity, causes mitochondrial PTEN-L accumulation for destabilising its structure via MFN1 for apoptosis. Consistent with this, VO prevented the cleavage and activation of caspase-3 upon ethanol exposure, in vivo (Fig. 7j, k). It also prevented the development of cardiac hypertrophy during chronic alcohol consumption
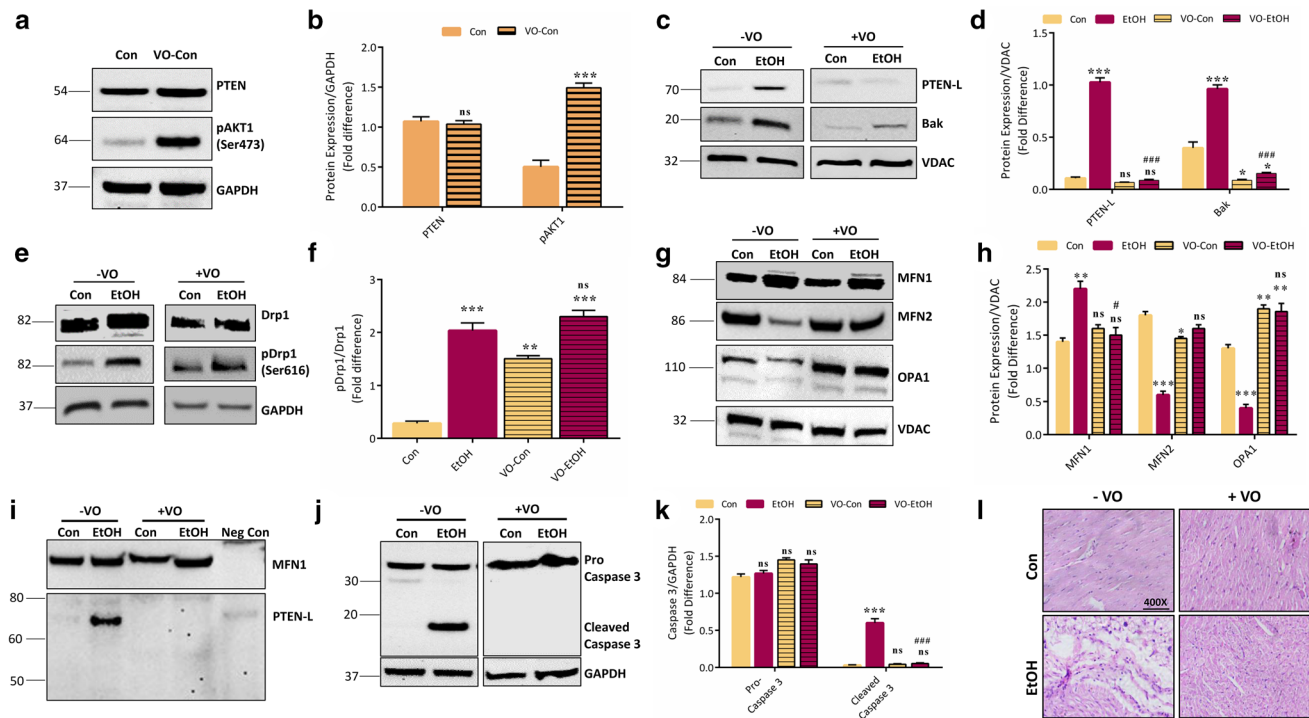
Fig. 7 In vivo inhibition of PTEN phosphatase ameliorates alcohol-induced cardiotoxicity. **a** Western blot demonstrating increased cardiac pAkt levels in VO pre-treated animals. **b** Quantitative representation of protein expression changes normalised to GAPDH. **c** VO pre-treatment prevented mitochondrial Bak and PTEN-L localisation during ethanol treatment. **d** Quantification of western blot in **c**. **e** Sustained pDrp1 levels in VO treated animals exposed to ethanol. **f** Quantification of western data in **e**. **g** Expression profile of mitochondrial fusion proteins in VO treated animals. **h** Quantification of western data in **g**. **i** Immunoprecipitation of PTEN-L with MFN1 antibody in ethanol treated animals. **j** VO prevented activation of caspase 3 for apoptosis. **k** Quantification of caspase-3 western blot data in **j**. **l** Histological assessment (H&E staining) of heart sections showing VO pre-treatment prevented hypertrophy of cardiomyocytes. Statistical significance was determined via student's t test and one-way ANOVA and data are represented as mean±SEM where ***$P < 0.001$, **$P < 0.01$, *$P < 0.05$, ns not significant versus respective control group and ##$P < 0.01$, #$P < 0.05$, ns not significant versus ethanol treated group

as seen upon histological examination of heart tissue sections (Fig. 7k). Ethanol-induced foamy macrophages in heart marking early stages of atherosclerotic lesion formation was not seen in VO pre-treated animals. Furthermore, VO increased antioxidant levels in control and ethanol treated animals compared to VO untreated animals (Supplementary Fig. 6A) complementing the reduced lipid peroxidation levels seen (Supplementary Fig. 6B).

Thus, data from this part of the study demonstrate PTEN-L interaction with MFN1 on the mitochondria, for Bak-mediated MOMP, can cause apoptosis and that preventing PTEN-L accumulation on the mitochondria is critical for improving resistance to alcohol.

Discussion

In this study, using in vivo and in vitro models, we show that chronic alcohol consumption promotes cardiac mitochondrial fragmentation and dysfunction, leading to cell death. During exposure to ethanol, cardiomyoblasts underwent apoptosis even in the absence of mitochondrial fission protein, Drp1, mediated by PTEN-L accumulation in the mitochondria for Bak-mediated MOMP and cytochrome c release. This was corroborated with in vivo experiments, where global inhibition of PTEN activity prevented mitochondrial PTEN-L-MFN1 interaction for organelle dysfunction, conferring resistance to alcohol-induced toxicity.

For this study, H9c2 cardiomyoblast cell line was chosen as in vitro model [54] as culturing of primary adult cardiomyocytes impacts mitochondrial fusion/fission dynamics [9]. Ethanol exposure triggered mitochondrial fragmentation in H9c2 cells and increased phosphorylation and mitochondrial localisation of fission protein Drp1. While we did see an increase in total Drp1 levels in animals treated with ethanol, this effect was not observed in H9c2 cells. It is possible that this could be due to the different cell types in the total heart tissue in comparison to exclusively cultured cardiomyoblasts used for in vitro analysis. Other mitochondrial fission factors like Mff, Fis1 and MiD49 did not show expression difference

Fig. 8 Graphical representation depicting PTEN-L as the central molecule that balances mitochondrial phase of cell death and cell survival during ethanol toxicity in the heart
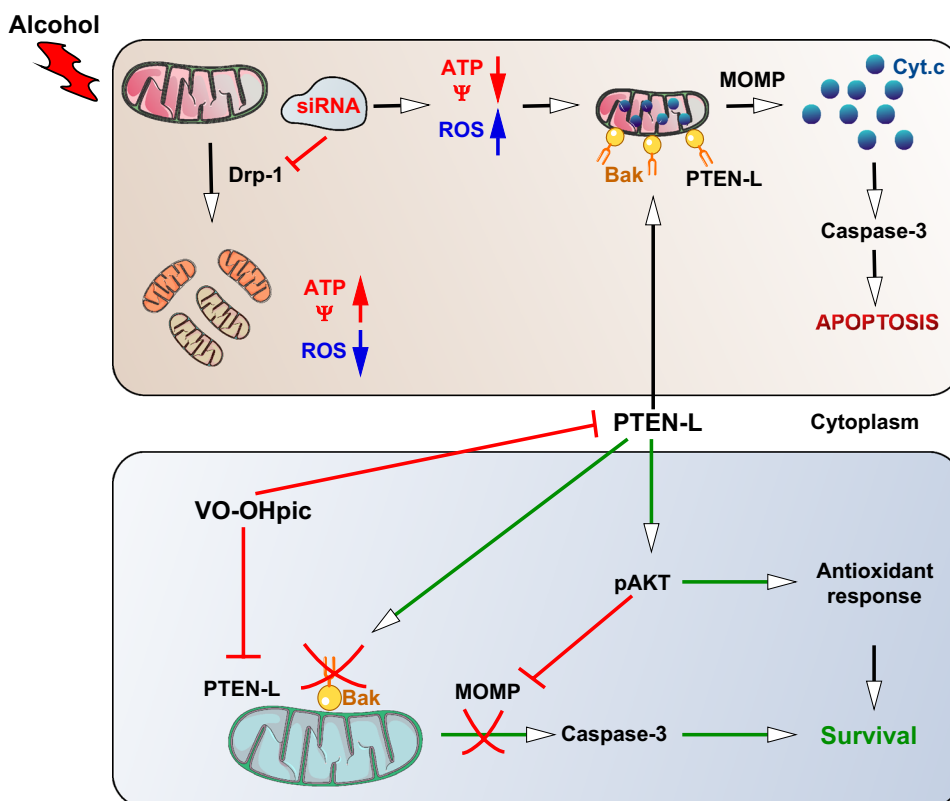
upon ethanol exposure but MiD51 was significantly lowered. Mitochondrial outer membrane resident MiD51 is reported to negatively influence Drp1 fission action on the membrane and to promote fusion [55]. Decreased expression of the same upon ethanol treatment could also have additional influence on destabilising mitochondrial structural dynamics and functional capacity in the heart.

Drp1 knockdown experiments were performed to understand the role of mitochondrial fragmentation in the organelle dysfunction and apoptosis. In vitro silencing of *Drp1* enhanced sensitivity to alcohol by increasing oxidative stress and downregulating the mitochondrial fusion proteins, MFN2 and OPA1. Consistent with this, our cell fractionation studies confirmed the accumulation of Bak in the mitochondria for OPA1 isoform dyshomeostasis [56], and cause release of cytochrome c from the mitochondria into the cytoplasm [57–61]. After establishing that oxidative stress is the cause of apoptosis during *Drp1* knockdown (using the antioxidant resveratrol), we attempted to reveal whether Drp1 is required for ethanol-mediated cytotoxicity. In doing so, we focused on analysing the following three mechanisms: (1) PTEN/Akt signalling in response to oxidative stress, (2) PTEN-L-MFN1 interaction, and (3) interlink between Drp1 and PTEN-L.

Previous studies show increased expression and/or activity of PTEN is seen in liver, neurons of developing brain and in utero of chronic alcohol ingested animals, with subsequent

decreased phosphorylation of Akt or increased association between PTEN and PI3K [62–66]. While we observed significant change in PTEN levels between scramble and Drp1 knockdown cells treated with ethanol, the function of differential expression of PTEN-L in stress conditions were analysed due to its mitochondrial localisation. We confirmed significant levels of PTEN-L in the mitochondria of ethanol treated cells, both scramble and *Drp1* silenced, in addition to its accumulation in untreated Drp1 knockdown cells. Preventing the mitochondrial PTEN-L accumulation with VO treatment markedly reduced Bak insertion, cytochrome c release and caspase-3 activation in both scramble and Drp1 knockdown cells, with or without ethanol treatment, confirming that PTEN-L in the mitochondrial can trigger the organelle's dysfunction. We also show evidence that precludes AKT-mediated protection upon PTEN inhibition by the sharp peak and fall in pAkt levels to normal upon prolonging the treatment.

Another important observation in the study is that PTEN-L interacts with MFN1 on the mitochondria as shown through our immunoprecipitation experiments. Protective effects seen upon VO treatment to ethanol consuming animals could be due to the undetectable levels of PTEN-L in the heart tissue. While we did observe upregulated pDrp1 levels both in vivo and in vitro upon VO pre-treatment, mitochondrial fusion proteins, MFN2 and OPA1, levels were restored with concomitant decrease in oxidative stress. Two

possible can be conclusions drawn from these observations: First, PTEN-L is a required component of MFN1-Bak signalling for apoptosis. Second, mitochondrial fragmentation could be the result of apoptosis rather than the cause. This corroborates with the Pink1-Parkin mitophagy associated functions of PTEN-L for eliminating dysfunctional mitochondria [67] and sustaining the energy demands of the cells.

In summary (Graphical representation Fig. 8), our study identifies PTEN-L as a key protein for apoptosis signalling when mitochondrial fragmentation is the result, rather than the cause of apoptosis, as that seen during ethanol induced cardiotoxicity. Thus, PTEN-L dynamics between mitochondria and cytoplasm is critical for the organelle's homeostasis. In addition, the study also identifies VO–OHpic as a potential therapeutic molecule for myocardial heath in habitual alcoholics.

Author contributions RS, AS—concept, design of experiments; AS, SS—execution of experiments, AS, RB—in vivo experiments; AS—data analysis and manuscript writing; RS,AS,SS,RB-Manuscript corrections and review.

Compliance with ethical standards

Conflict of interest The authors declare no conflict of interest.

References

1. Fernandez-Sola J (2015) Cardiovascular risks and benefits of moderate and heavy alcohol consumption. Nat Rev Cardiol 12:576–587
2. Hvidyfeldt UA et al (2010) Alcohol intake and risk of coronary heart disease in younger, middle-aged, and older adults. Circulation 121:1589–1597
3. Piano MR (2002) Alcohol and heart failure. J Card Fail 8:239–246
4. Guzzo-Merello G, Cobo-Marcos M, Gallego-Delgado M, Garcia-Pavia P (2014) Alcoholic cardiomyopathy. World J Cardiol 6:771–781
5. Piano MR (2002) Alcoholic cardiomyopathy: incidence, clinical characteristics and pathophysiology. Chest 121:1638–1650
6. Umoh NA, Walker RK, Al-Rubaiee M, Jeffress MA, Haddad GE (2014) Acutre alcohol modulates cardiac function as PI3K/Akt regulates oxidative stress. Alcohol Clin Exp Res 38:1847–1864
7. Ong SB et al (2015) Akt protects the heart against ischaemia-reperfusion injury by modulating mitochondrial morphology. Thromb Haemost 113:513–521
8. Sudarikova YV, Bakeeva LE, Tsiplenkova VG (1997) Ultrastructure of mitochondrial reticulum of human cardiomyocytes in alcohol cardiomyopathy. Biochemistry (Mosc) 62:989–1002
9. Eisner V et al (2017) Mitochondrial fusion dynamics is robust in the heart and depends on calcium oscillations and contractile activity. Proc Natl Acad Sci USA 114:E859–E896
10. Sivakumar A, Subbiah R, Balakrishnan R, Rajendhran J (2017) Cardiac mitochondrial dynamics: miR-mediated regulation during cardiac injury. J Mol Cell Cardiol 110:26–34
11. Song M, Mihara K, Chen Y, Scorrano L, Dorn GW 2nd (2015) Mitochondrial fission and fusion factors reciprocally orchestrate mitophagic culling in mouse hearts and cultured fibroblasts. Cell Metab 21:273–286
12. Youle RJ, van der Bliek AM (2012) Mitochondrial fission, fusion and stress. Science 337:1062–1065
13. Ong SB, Kalkhoran SB, Cabrera-Fuetnes HA, Hausenloy DJ (2015) Mitochondrial fusion and fission proteins as novel therapeutic targets for treating cardiovascular disease. Eur J Pharmacol 763:104–114
14. Smirnova E, Griparic L, Shurland DL, van der Bliek AM (2001) Dynamin-related protein Drp1 is required for mitochondrial division in mammalian cells. Mol Biol Cell 12:2245–2256
15. Smirnova E, Shurland DL, Ryazantsev SN, van der Bliek AM (1998) A human dynamin-related protein controls the distribution of mitochondria. J Cell Biol 143:351–358
16. Yoon Y, Krueger EW, Oswald BJ, McNiven MA (2003) The mitochondrial protein hFis1 regulates mitochondrial fission in mammalian cells through an interaction with the dynamin-like protein DLP1. Mol Cell Biol 23:5409–5420
17. Ong SB, Subrayan S, Lim SY, Yellon DM, Davidson SM, Hausenloy DJ (2010) Inhibiting mitochondrial fission protects the heart against ischemia/reperfusion injury. Circulation 121:2012–2022
18. Sharp WW et al (2014) Dynamin-related protein 1 (Drp1)-mediated diastolic dysfunction in myocardial ischemia-reperfusion injury: therapeutic benefits of Drp1 inhibition to reduce mitochondrial fission. FASEB J 28:316–326
19. Pennanen C et al (2014) Mitochondrial fission is required for cardiomyocyte hypertrophy mediated by a Ca2+-calcineurin signalling pathway. J Cell Sci 127:2659–2671
20. Din S et al (2013) Pim-1 preserves mitochondrial morphology by inhibiting dynamin-related protein 1 translocation. Proc Natl Acad Sci USA 110:5969–5974
21. Watanabe T et al (2014) Roles of mitochondrial fragmentation and reactive oxygen species in mitochondrial dysfunction and myocardial insulin resistance. Exp Cell Res 323:314–325
22. Disatnik MH et al (2013) Acute inhibition of excessive mitochondrial fission after myocardial infarction prevents long-term cardiac dysfunction. J Am Heart Assoc 2:e000461
23. Pushpakiran G, Mahalakshmi K, Anuradha CV (2004) Taurine restores ethanol-induced depletion of antioxidants and attenuates oxidative stress in rat tissues. Amino Acids 27:91–96
24. Zu L, Shen Z, Wesley J, Cai ZP (2011) PTEN inhibitors cause a negative inotropic and chronotrophic effect in mice. Eur J Pharmacol 10:298–302
25. Ramasamy S, Velmurugan G, Rekha B, Anusha S, Rajan KS, Shanmugarajan S, Ramprasath T, Gopal P, Tomar D, Karthik KV, Verma SK, Garikipati VNS, Sudarsan R (2018) Egr-1 mediated cardiac miR-99 family expression diverges physiological hypertrophy from pathological hypertrophy. Exp Cell Res 365:46–56
26. Bradford MM (1976) A rapid and sensitive method for the quantification of microgram quantities of protein utilising the principle of protein-dye binding. Anal Biochem 72:248–254
27. Ohkawa H, Ohishi N, Yagi K (1979) Assay for lipid peroxides in animal tissues by thiobarbituric acid reaction. Anal Biochem 95:351–358
28. Ila R, Solem M (2006) Chronic alcohol exposure alters IGF1 signaling in H9c2 cells via changes in PKC delta. Alcohol 39:169–178
29. Mak LH, Vilar R, Woscholski R (2010) Characterisation of the PTEN inhibitor VO-OHpic. J Chem Biol 3:157–163

30. Okada M, Morioka S, Kanazawa H, Yamawaki H (2016) Canstatin inhibits isoproterenol-induced apoptosis through preserving mitochondrial morphology in differentiated H9c2 cardiomyoblasts. Apoptosis 21:887–895

31. Gostimskaya I, Galkin A (2010) Preparation of highly coupled rat heart mitochondria. J Vis Exp 43:2202

32. Frezza C, Cipolat S, Scorrano L (2007) Organelle isolation: functional mitochondria from mouse liver, muscle and cultured fibroblasts. Nat Protoc 2:287–295

33. Rekha B et al (2018) Chronic intaking of 4-methyimidazole induces hyperinsulinemia and hypoglycaemia via pancreatic beta cell hyperplasia and glucose dyshomeostasis. Sci Rep 8:17037

34. Brandt N et al (2017) PGC-1α and exercise intensity dependent adaptations in mouse skeletal muscle. PLoS ONE 12:e0185993

35. Wu S, Zhou F, Zhang Z, Xing D (2011) Mitochondrial oxidative stress causes mitochondrial fragmentation via differential modulation of mitochondrial fission-fusion proteins. FEBS J 278:941–954

36. Mashimo K, Arthur PG, Ohno Y (2015) Ethanol dose- and time-dependently increases alpha and beta subunits of mitochondrial ATP Synthase of cultured neonatal rat cardiomyocytes. J Nippon Med Sch 82:237–245

37. Marin-Garcia J, Ananthakrishnan R, Goldenthal MJ (1995) Heart mitochondria response to alcohol is different than brain and liver. Alcohol Clin Exp Res 19:1463–1466

38. Ikeda Y, Shirakabe A, Brady C, Zablocki D, Ohishi MM, Sadoshima J (2015) Molecular mechanisms mediating mitochondrial dynamics and mitophagy and their functional roles in the cardiovascular system. J Mol Cell Cardiol 78:116–122

39. Song Z, Chen H, Fiket M, Alexander C, Chan DC (2007) OPA1 processing controls mitochondrial fusion and is regulated by mRNA splicing, membrane potential and Yme1L. J Cell Biol 178:749–755

40. Zhou LL, Zhou LY, Luo KQ, Chang DC (2005) Smac/DIABLO and cytochrome c are released from mitochondria through a similar mechanism during UV-induced apoptosis. Apoptosis 10:289–299

41. Legros F, Lombes A, Frachon P, Rojo M (2002) Mitochondrial fusion in human cells is efficient, requites the inner membrane potential and is mediated by the mitofusins. Mol Biol Cell 13:4343–4354

42. Guo S, Yao Q, Ke Z, Chen H, Wu J, Liu C (2015) Resveratrol attenuates high glucose-induced oxidative stress and cardiomyocyte apoptosis through AMPK. Mol Cell Endocrinol 412:85–94

43. Fang WJ, Wang CJ, He Y, Zhou YL, Peng XD, Liu SK (2018) Resveratrol alleviates diabetic cardiomyopathy in rats by improving mitochondrial function through PGC-1α deacetylation. Acta Pharmacol Sin 39:59–73

44. Movahed A, Yu L, Thandapilly SJ, Louis XL, Netticadan T (2012) Resveratrol protects adult cardiomyocytes against oxidative stress mediated cell injury. Arch Biochem Biophys 527:74–80

45. Biala A et al (2010) Resveratrol induces mitochondrial biogenesis and ameliorates Ang- II-induced cardiac remodelling in transgenic rats harbouring human renin and angiotensinogen genes. Blood Press 19:196–205

46. Walker RK et al (2013) The good, the bad, and the ugly with alcohol use and abuse on the heart. Acohol Clin Exp Res 37:1253–1260

47. Sag CM, Santos CX, Shah AM (2014) Redox regulation of cardiac hypertrophy. J Mol Cell Cardiol 73:103–111

48. Hopkins BD et al (2014) A secreted PTEN phosphatase that enters cells to alter signalling and survival. Science 341:399–402

49. Vela L, Gonzalo O, Naval J, Marzo I (2013) Direct interaction of Bax and Bak proteins with Bcl-2 homology domain 3 (BH3)-only proteins in living cells revealed by fluorescence complementation. J Biol Chem 288:4935–4946

50. Estaquier J, Arnoult D (2007) Inhibiting Drp1-mediated mitochondrial fission selectively prevents the releaseo f cytochrome c during apoptosis. Cell Death Differ 14:1086–1094

51. Parone PA et al (2006) Inhibiting the mitochondrial fission machinery does not prevent Bax/Bak-dependent apoptosis. Mol Cell Biol 26:7397–7408

52. Madesh M et al (2009) Execution of superoxide-induced cell death by the proapoptotic Bcl-2 related proteins Bid and Bak. Mol Cell Biol 29:3099–3112

53. Brooks C et al (2007) Bak regulates mitochondrial morphology and pathology during apoptosis by interacting with mitofusins. Proc Natl Acad Sci USA 104:11649–11654

54. Hescheler J, Meyer R, Plant S, Krautwurst D, Rosenthal W, Schultz G (1991) Morphological, biochemical, and electrophysiological characterisation of a clone cell (H9c2) line from rat heart. Circ Res 69:1476–1486

55. Zhao J et al (2011) Human MIEF1 recruits Drp1 to mitochondrial outer membranes and promotes mitochondrial fusion rather than fission. EMBO J 30:2762–2778

56. Jiang X, Jiang H, Shen Z, Wang X (2014) Activation of mitochondrial protease OMA1 by Bax and Bak promotes cytochrome c release during apoptosis. Proc Natl Acad Sci USA 111:14782–14787

57. Arnoult D, Grodet A, Lee YJ, Estaquier J, Blackstone C (2005) Release of OPA1 during apoptosis participates in the rapid and complete release of cytochrome c and subsequent mitochondrial fragmentation. J Biol Chem 280:35742–35750

58. Griparie L, van der Wel NN, Orozco IJ, Peters PJ, van der Bliek AM (2004) Loss of intermembrane space protein Mgm1/OPA1 induces swelling and localised constrictions along the lengths of mitochondria. J Biol Chem 279:18792–18798

59. Tang S, Le PK, Tse S, Wallace DC, Huang T (2009) Heterozygous mutation of Opa1 in Drosophila shortens lifespan mediated through increased reactive oxygen species production. PLoS ONE 4:e4492

60. Olichon A et al (2003) Loss of OPA1 perturbates the mitochondrial inner membrane structure and integrity, leading to cytochrome c release and apoptosis. J Biol Chem 278:7743–7746

61. Chen L, Gong Q, Stice JP, Knowlton AA (2009) Mitochondrial OPA1, apoptosis and heart failure. Cardiovasc Res 84:91–99

62. Lu C et al (2015) Attenuation of cardiac dysfunction and remodelling of myocardial infarction by microRNA-130a is mediated by suppression of PTEN and activation of Pi3K dependent signalling. J Mol Cell Cardiol 89:87–97

63. Yeon JE, Califano S, Xu J, Wands JR, De La Monte SM (2003) Potential role of PTEN phosphatase in ethanol-impaired survival signalling in the liver. Hepatology 38:703–714

64. Xu J et al (2003) Ethanol impairs insulin-stimulated neuronal survival in the developing brain: Role of PTEN phosphatase. J Biol Chem 278:26929–26937

65. Yao XH, Nyomba BL (2008) Hepatic insulin resistance induced by prenatal alcohol exposure is associated with the reduced PTEN and TRB3 acetylation in adult rat offspring. Am J Physiol Regul Integr Comp Physiol 294:R1797–1806

66. He J, de la Monte S, Wands JR (2007) Acute ethanol exposure inhibits insulin signalling in the liver. Hepatology 46:1791–1800

67. Wang L et al (2018) PTEN-L is a novel protein phosphatase for ubiquitin dephosphorylation to inhibit PINK1-Parkin-mediated mitophagy. Cell Res 28:787–802